24468 : 840597

U.S. Department
of Transportation
**National Highway
Traffic Safety
Administration**

629.2042
I61
1989
v.2

8-23-90

The Twelfth International Technical Conference on Experimental Safety Vehicles

Sponsored by:
U.S. Department of Transportation
National Highway Traffic Safety Administration

Hosted by:
Swedish Government

Held at:
Göteborg, Sweden
May 29—June 1, 1989

results are to be generalized over a broad range of operating conditions (this is not the case for the first four methods, where all testing can be done on one high-mu surface). Constructing and maintaining several surfaces f r testing can be a very costly proposition, but it offers a very realistic condition in terms of how the consumer will operate the vehicle. Tire/road peak mu and brake application time must be known in order to calculate braking efficiency from stopping distance, but this value may differ from braking efficiency derived from the first four methods because of vehicle suspension effects and road roughness.

The Annex 13 approach to measuring efficiency is flawed in its technique for measuring tire/road coefficient or friction. If this problem is corrected the approach may be viable, but as is the case with stopping distance approach, a number of surfaces will be required to cover a range of braking rates. Also, for the reasons given above, the approach will not necessarily produce the same braking efficiency as the brake force measurement-based methods.

References

(1) Radlinski, Richard W. and Flick, Mark A., "A Vehicle Test Pr cedure for Determining Adhesi n Utilization Properties," SAE Paper No. 840334, 1984.

(2) Wolanin, Michael J. and Baptist, Thomas A. "Road Transducer—Objective Brake Balance Measurement Without Vehicle Instrumentation," SAE Paper No. 870266, February 1987.

(3) Flick, Mark A. and Radlinski, Richard W., "Harmonization of Braking Regulations—Report Number 6: Testing to Address Surface Friction and Vehicle Braking Efficiency Comments to the SNPRM," Vehicle Research and Test Center, Final Report No. DOT HS 807 393, March 1989.

Dynamic Analysis of Vehicle Rollover

Andrzej G. Nalecz and Alan C. Bindemann,
University of Missouri-Columbia
Howell K. Brewer,
National Highway Traffic Safety Administration

Abstract

Statistical analyses of collected accident data have shown that incidents involving rollover represent a major safety concern based on both the frequency of occurrence and the severity level of occupant injury. Computer based models can be used to provide valuable insight into the dynamic behavior of vehicle rollover and determine the influence of basic vehicle design parameters on vehicle rollover propensity. This paper describes two computer based models which can be used to investigate vehicle rollover. The first of these models represents the Intermediate Tripped Rollover Simulation (ITRS). This computer simulation is capable of determining the response of a vehicle which slides laterally into a rigid curb, initiating vehicle rollover. The second model is the Intermediate Maneuver Induced Rollover Simulation (IMIRS) and is used to investigate untripped vehicle rollover accidents caused by sudden or excessive steering and braking inputs. Results obtained from each model are shown and general purpose sensitivity methods are applied to each model in order to investigate the relative influence of various vehicle design parameters on vehicle rollover propensity. The use of Rollover Prevention Energy Reserve (RPER) as a measure of vehicle stability is explained and demonstrated using each model.

Introduction

Accidents involving vehicle rollover have b en and continue to be one of the most hazardous types of vehicle accidents. Th serious nature of the rollover problem is documented in the various collections of rollover accident data compiled by the National Highway Traffic Safety Administration (NHTSA) (1–4)*. According to data collected from the Fatal Accident Reporting System (FARS) rollover was identified as being a factor in over 20 percent of all non-collision fatalities in single vehicle accidents which occurred in 1986. Data collected using the National Accident Sampling System (NASS) in 1985 shows that 20 percent of the 18,400 fatalities which occurred that year were in accidents involving rollover, while at the same time, rollover occurred in less than 7 percent of all accidents. Several studies of accident data show a strong correlation between vehicle size and/or type and the likelihood of its involvement in a rollover accident (5–12). A report by Snyder et al. (6) shows that utility vehicles have the highest likelihood of rolling over in an accident. Other reports indicate that small utility vehicles, those having a wheelbase which is less than 100 inches, have the highest number of occupant deaths per 10,000 vehicles registered. The Insurance Institute for Highway Safety (IIHS) has concluded that the major reason behind this high death rate is associated with the propensity of small utility vehicles to rollover and eject occupants in an accident. The Institute study attributes 46 percent of all occupant deaths associated with utility vehicles to single vehicle accidents which involve rollover with ejection (7). The Institute also found that the fatality rate due to rollover in single vehicle accidents of light pickup trucks, those weighing less than 3200 pounds, and intermediate utility vehicles, those with a wheel base between 100 and 120 inches, is substantially higher than the rates associated with the different classes of passenger cars. The fatality rate associated with passenger cars in rollover accidents was found to decrease as vehicle size increased.

*Numbers in parentheses designate references at end of paper.

Because accidents which involve rollover occur frequently and typically impart serious injuries to vehicle occupants it is both beneficial and necessary to investigate and identify the factors which contribute to rollover. In general, these issues might be related to human factors such as age, alcohol involvement, or driver reaction in an accident situation; they might also be related to environmental factors such as pavement conditions, curb profile, and embankment conditions. Finally they may be related to factors associated with vehicle design such as track width, suspension geometry, and minimum acceptable ground clearance. Research into each of these safety issues is imperative since utility vehicles and light pickup trucks make up a growing share of the American new car market and the domestic passenger car fleet continues to undergo a rapid reduction in size and weight. The results of such investigations can be used to lower the number of rollover accidents and to find ways to mitigate occupant injuries when rollovers do occur.

A considerable amount of research into the factors which influence rollover propensity attempts to find correlations between vehicle parameters such as weight, wheelbase, and track width with rollover statistics from accident data bases compiled by organizations such as NHTSA and IIHS. The Texas Transportation Research Institute (8, 9) examined rollover risk of passenger cars as a function of road type and vehicle weight and found that vehicle rollover did increase with decreasing vehicle weight. However, this study could not make any conclusions relating vehicle weight to the dynamic behavior associated with rollover since weight could simply correlate with one or more vehicle parameters such as track width, wheelbase or moments of inertia.

There have also been numerous experimental studies of rollover behavior. Habberstad, Wagner and Thomas (13) investigated the influence of occupant ejection and roof crush on occupant injury in a tripped rollover test. Calspan Corporation (14) examined the rollover behavior of a Volkswagen Rabbit on a sloping soil embankment in order to determine the effect of roadside features on rollover propensity. Prompted by litigation, American Motors Corporation performed both tripped and untripped rollover tests on a variety of vehicles in an effort to demonstrate that a wide range of vehicles could be made to rollover. More recently, several experimental tests have been performed to demonstrate the rollover stability of several popular utility vehicles. While tests of this nature can sometimes provide useful information, they frequently provide inadequate information regarding test conditions and are not always sponsored or performed by totally impartial organizations; therefore these tests must be examined critically.

Experimental tests can provide useful knowledge on the dynamic behavior of rollover accidents, but like statistical tests, they are poorly suited for determining the influence of vehicle design parameters on rollover behavior since it is often difficult t vary vehicle parameters one at a time. Experimental repeatability is also an extremely important when trying to access the influence of different design parameters. Finally, the high costs associated with full scale rollover testing can preclude extensive parametric investigation.

Analytical investigation into the dynamic behavior of vehicles is the most effective method of determining the influence of design parameters on vehicle response. While analytical methods have found only limited use in the investigation of human factors, these methods are quite useful in the study of environmental and design factors. Computer based simulation models can be used to predict vehicle response in a variety of conditions, gain insight into the fundamental reasons behind dynamic phenomenon such as rollover, and provide information on the influence of design parameters on dynamic response.

There have been numerous analytical studies into the causes of vehicle rollover. Jones of Calspan Corporation (15) analyzed the mechanics of rollover as the result of curb impact. Calspan (16) also used its Highway Vehicle Object Simulation Model (HVOSM) to investigate the influence of roadway features on rollover. Systems Technology Incorporated (STI) (17) developed a tripped rollover model which simulated response of a vehicle which slides laterally into a curb. Later the University of Missouri-Columbia (18) used this model to analyze the influence of design parameter variations on rollover response using sensitivity models.

This paper presents an overview of current rollover research sponsored by NHTSA and being performed at the University of Missouri-Columbia. The Intermediate Tripped Rollover Simulation (ITRS) is described and demonstrated for the cases of simultaneous and oblique curb impacts. An energy based rollover stability measure known as Rollover Prevention Energy Reserve (RPER) is introduced and the influence of basic vehicle design parameters on this measure is determined using sensitivity methods. The paper also illustrates the Intermediate Maneuver Induced Rollover Simulation (IMIRS). This model can be used to investigate the rollover propensity of vehicles which are subjected to severe cornering and braking accelerations. Results obtained from the IMIRS simulation in J and S turn maneuvers are presented. Sensitivity methods are used to determine the influence of several basic vehicle design parameters on a dynamic measure of rollover stability. Finally, the paper describes the development of the Advanced Vehicle Rollover Model (AVRM).

Intermediate Tripped Rollover Simulation

An extensive review of accident statistics has shown that a majority of vehicle rollovers are initiated by an excursion into a roadside feature such as a curb, ditch, or embankment. M st frequently, a driver loses control of the vehicle and it skids at a large sideslip angle when it strikes or crosses the tripping roadside feature. Vehicle contact with these roadside discontinuities can result in high levels of deceleration that generate large inertia forces which act on

the vehicle. These inertia forces generate rolling moments about the roadside discontinuity and if these moments exceed inertia couples and gravitational forces which resist vehicle roll then the vehicle will leave a four wheel stance and can rollover. The purpose of the Intermediate Tripped Rollover Simulation (ITRS) is to investigate the tripped rollover motion of a vehicle which slides into a curb. The simulation permits investigation of impacts at different sideslip angles as well as different angles of incidence with the curb. The ITRS has been used extensively to investigate rollover behavior by examining the energy exchange which occurs in tripped rollover situations.

A moderate level of detail was used during the formulation of the ITRS. This represented a compromise between an overly simplistic model which would be incapable of examining the influence of vehicle subsystem design on rollover propensity, and a highly detailed model, which would require that extensive vehicle measurements be performed in order to obtain the data required to drive the simulation. Also, because there is very little experimental investigation into the impact forces which occur when the tire and wheel contact a roadside feature it is unrealistic to develop highly detailed vehicle models until more is known about these impact forces.

Work on the ITRS was initiated after performing a sensitivity analysis (18) of an existing tripped rollover simulation (17). This rollover simulation program was intended to investigate the rollover behavior of a vehicle which was skidding, at a sideslip angle of 90 degrees, into a curb. The simulation permitted small variations in the heading angle of the vehicle as measured relative to the curb at the instant of impact. After performing the sensitivity analysis of this model it was decided that an improved tripped rollover model should be developed based on the previous one. Improvements in this new model include the addition of forward dynamics, the inclusion of all dynamic couplings in the equations of motion and the addition of a more sophisticated curb impact model. These additions permit investigation of tripped rollover accidents over a full range of vehicle sideslip angles and incidence angles with the curb.

ITRS model description

The ITRS simulation utilizes an 8 degree of freedom model to represent the vehicle. The model (figure 1) consists of two masses, one representing the vehicle's sprung mass and a second mass which represents the combined unsprung masses of front and rear suspension systems. The masses are connected using two pins attached to the front and rear of the sprung mass which can slide in vertical slots located in the unsprung mass. The pins permit the sprung mass to move vertically relative to the unsprung mass and also allow relative rotation between the two masses. The pins represent the vehicle roll axis, whose position is determined from the kinematics of the front and rear suspension systems. The suspension model assumes that the vehicle's roll axis is parallel to the ground and lies in the vehicle's plane of symmetry at all times. The sprung mass is attached to the unsprung mass using four springs and four viscous dampers. There are also four upper bump stops and four lower bump stops attached to the unsprung mass to prevent excessive relative motion between both masses. Each bump stop consists of an elastic element placed in parallel with a viscous damping element. The suspension model is illustrated in figure 1.

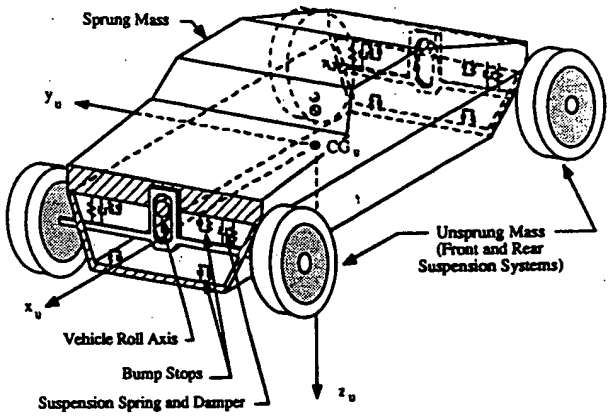

Figure 1. The ITRS vehicle model and non-inertial reference system assumed.

No planes of symmetry were assumed in the analysis, therefore all elements of the inertia matrices describing the sprung and unsprung masses were included in the equations of motion. The degrees of freedom include three angles of rotation and three linear translations of the unsprung mass, the vertical position of the sprung mass, and the roll angle of the sprung mass. The model assumes that the pitch and yaw angles of the two masses are identical. The following eight generalized coordinates are used in the model.

$q1 = x$ longitudinal position of unsprung mass c.g. in the absolute reference system

$q2 = y$ lateral position of unsprung mass c.g. in the absolute reference system

$q3 = z_u$ vertical position of unsprung mass c.g. in the absolute reference system

$q4 = z_s$ vertical position of sprung mass roll axis in the absolute reference system

$q5 = \phi u$ unsprung mass roll angle

$q6 = \phi s$ sprung mass roll angle

$q7 = \theta$ vehicle pitch angle

$q8 = \Psi$ vehicle yaw angle

Equations of motion

The equations of motion for the ITRS model were formulated using the Newton-Euler approach. Provided the origin of the non-inertial reference system attached to the rigid body (point P) is located at the body's center of mass (i.e. $\bar{P}_c = 0$) or is not accelerating, the rigid body equations of motion can be written in the following form:

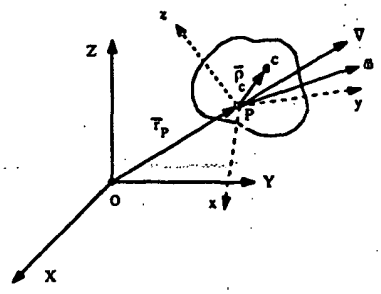

Figure 2. General rigid body motion.

$$F_x = m(\dot{v}_x + v_z\omega_y - v_y\omega_z)$$

$$F_y = m(\dot{v}_y + v_x\omega_z - v_z\omega_x)$$

$$F_z = m(\dot{v}_z + v_y\omega_x - v_x\omega_y) \qquad (1)$$

$$M_x = I_{xx}\dot{\omega}_x + I_{xy}(\dot{\omega}_y - \omega_x\omega_z) + I_{xz}(\dot{\omega}_z + \omega_x\omega_y) + (I_{zz} - I_{yy})\omega_y\omega_z + I_{yz}(\omega_y^2 - \omega_z^2)$$

$$M_y = I_{yy}\dot{\omega}_y + I_{xy}(\dot{\omega}_x + \omega_y\omega_z) + I_{yz}(\dot{\omega}_z + \omega_x\omega_y) + (I_{xx} - I_{zz})\omega_x\omega_z + I_{xz}(\omega_z^2 - \omega_x^2)$$

$$M_z = I_{zz}\dot{\omega}_z + I_{yz}(\dot{\omega}_y + \omega_x\omega_z) + I_{xz}(\dot{\omega}_x - \omega_y\omega_z) + (I_{yy} - I_{xx})\omega_x\omega_y + I_{xy}(\omega_x^2 - \omega_y^2)$$

If the origin of the non-inertial reference system does not satisfy either one of the two conditions listed above then the Newton-Euler equations of motion must be extended to the following form:

$$F_x = m\left[\dot{V}_{P_x} + V_{P_z}\omega_y - V_{P_y}\omega_z + \rho_x\dot{\omega}_y - \rho_y\dot{\omega}_z + \omega_y(\omega_x\rho_y - \omega_y\rho_x) - \omega_z(\omega_z\rho_x - \omega_x\rho_z)\right]$$

$$F_y = m\left[\dot{V}_{P_y} + V_{P_x}\omega_z - V_{P_z}\omega_x + \rho_x\dot{\omega}_z - \rho_z\dot{\omega}_x + \omega_z(\omega_y\rho_z - \omega_z\rho_y) - \omega_x(\omega_x\rho_y - \omega_y\rho_x)\right]$$

$$F_z = m\left[\dot{V}_{P_z} + V_{P_y}\omega_x - V_{P_x}\omega_y + \rho_y\dot{\omega}_x - \rho_x\dot{\omega}_y + \omega_x(\omega_z\rho_x - \omega_x\rho_z) - \omega_y(\omega_y\rho_z - \omega_z\rho_y)\right] \qquad (2)$$

$$M_x = I_{xx}\dot{\omega}_x + I_{xy}(\dot{\omega}_y - \omega_x\omega_z) + I_{xz}(\dot{\omega}_z + \omega_x\omega_y) + (I_{zz} - I_{yy})\omega_y\omega_z + I_{yz}(\omega_y^2 - \omega_z^2) + m(\rho_y a_z - \rho_z a_y)$$

$$M_y = I_{yy}\dot{\omega}_y + I_{xy}(\dot{\omega}_x + \omega_y\omega_z) + I_{yz}(\dot{\omega}_z + \omega_x\omega_y) + (I_{xx} - I_{zz})\omega_x\omega_z + I_{xz}(\omega_z^2 - \omega_x^2) + m(\rho_z a_x - \rho_x a_z)$$

$$M_z = I_{zz}\dot{\omega}_z + I_{yz}(\dot{\omega}_y + \omega_x\omega_z) + I_{xz}(\dot{\omega}_x - \omega_y\omega_z) + (I_{yy} - I_{xx})\omega_x\omega_y + I_{xy}(\omega_x^2 - \omega_y^2) + m(\rho_x a_y - \rho_x a_y)$$

where, ρ_x, ρ_y and ρ_z represent the x, y, z components of the vector $\bar{P}_c$ and a_x, a_y and a_z are the x, y, z acceleration components of the non-inertial reference system origin (point P).

It should be noted that all velocity components in both sets of equations are measured in the non-inertial reference system. Also, in both sets of equations F_x, F_y, F_z, M_x, M_y, and M_z represent the x, y, z components of the external forces and moments which act on the rigid body as seen in the non-inertial reference system. In the case of interconnected multi-body systems, the bodies can be split apart and the Newton-Euler equations can be applied separately to each of the bodies. If this approach is used then the reactions which occur at the connections between the rigid bodies must be determined. Additional equations of motion obtained from separating the system into subsystems can be used to solve for the reactions which occur at the system connections.

The ITRS model is a multi-body dynamic system in which the first body represents the unsprung mass, and the second represents the sprung mass. These bodies are interconnected through the vehicle roll axis, and by numerous spring and damping elements which comprise the suspension system. The origin of the non-inertial reference system attached to the unsprung mass is located at the unsprung mass c.g. Therefore the first form of the Newton-Euler equations (1) of motion were used to formulate the equations of motion of the unsprung mass. The origin of the non-inertial reference system attached to the sprung mass is located in the same longitudinal plane as the sprung mass c.g., however, the longitudinal axis (the x axis) of the non-inertial reference system coincides with the vehicle roll axis, and does not pass through the c.g. of the sprung mass. Since the origin of this non-inertial reference system does not coincide with the sprung mass c.g., and the origin of the system is expected to accelerate, the second form of the Newton-Euler equations of motion (2) had to be used to formulate the sprung mass equations of motion. The resulting equations include all moments and products of inertia and also include all dynamic couplings.

External forces

The external forces which act on the vehicle include gravitational forces, the normal reactions at the wheels, the frictional forces of tires, and the impact forces which occur when the vehicle strikes the curb. The tire normal reactions are calculated using a linear spring and damping element. The normal reaction is dependent on the radial deformation of the tire, as well as the rate of radial tire deformation (index i = 1, ..., 4 is used to denote each of the four wheels):

$$F_{z_i} = K_z\Delta T_{r_i} - B_z\dot{\Delta T}_{r_i} \qquad \Delta T_{r_i} > 0$$

$$F_{z_i} = 0 \qquad \Delta T_{r_i} \le 0 \qquad (3)$$

The radial deformation of each tire is dependent on the vertical position, roll angle and pitch angle of the unsprung mass.

The x and y components of the tire frictional forces are computed using the following relations:

$$F_{xf_i} = \mu_x F_{z_i} f_x(v_{x_i})$$

$$F_{yf_i} = \mu_y F_{z_i} f_y(v_{y_i}) \qquad (4)$$

where, μ_x and μ_y are the sliding coefficients of friction of the

tire in the x and y directions and $f_x(v_{x_i})$, $f_y(v_{y_i})$ represent nonlinear functions of the tire sliding velocity. These functions are introduced to insure that the frictional forces act to oppose vehicle motion and prevent the sudden reversal of tire frictional forces if velocities v_{x_i} or v_{y_i} change signs. The form of functions $f_x(v_{x_i})$ and $f_y(v_{y_i})$ is shown in figure 3.

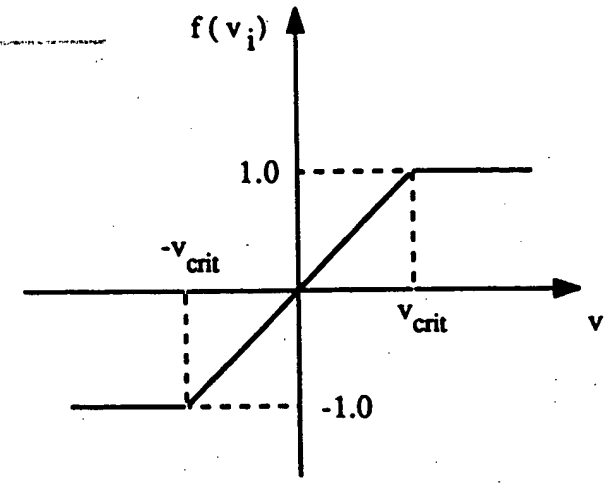

Figure 3. Velocity dependent tire frictional function.

The force which occurs when the tire comes into contact with the curb consists of two components, an impact force which is perpendicular to the curb, and a scrub force which acts parallel to the curb. The impact force is dependent on the amount of deformation as well as the time rate of change in the deformation. The deformation is determined based on the location and orientation of the vehicle relative to the curb. A force displacement curve having three linear slopes in three regions is used to determine the elastic portion of the impact force and is shown in figure 4. The first region of the force displacement curve is totally elastic and is used to represent wheel compliance. The second region represents a zone where plastic deformation occurs as the wheel and suspension elements undergo permanent crush. As the amount of deformation increases, more solid members of the vehicle such as the frame and powertrain are deformed and the third region of the curve is utilized. If the vehicle rebounds after impact the force displacement curve will unload using one of two slopes. If the deformation is totally elastic, i.e. in region I, then the force displacement curve will unload at slope K_1. If the deformation is plastic, i.e. in regions II or III, then the curve will unload at slope K_4. If plastic deformation does occur then the amount of permanent deformation is noted and the force deformation curve will reload using slope K_4 on subsequent impacts. Thus in subsequent impacts the impact force is computed as a function of previous plastic deformation.

The portion of the impact force which is dependent on the time rate of change in the deformation is modelled using a viscous damping characteristic. The force component which is dependent on deformation and the force component dependent on the rate of deformation are added together to obtain the total impact force.

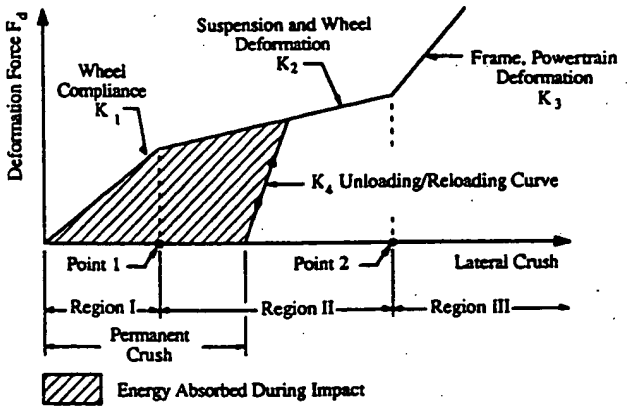

Figure 4. Force deflection characteristic used in the ITRS f r curb impact.

The scrub force which is generated during a curb impact is determined using the following relationship:

$$F_{scrub_i} = \mu_s F_{impact_i} f(vX_i) \qquad (5)$$

where, μ_s represents the tire friction coefficient along the curb, F_{impact_i} is the impact force normal to the curb, and $f(vX_i)$ represents a non-linear function of the tire's scrub velocity shown in figure 5.

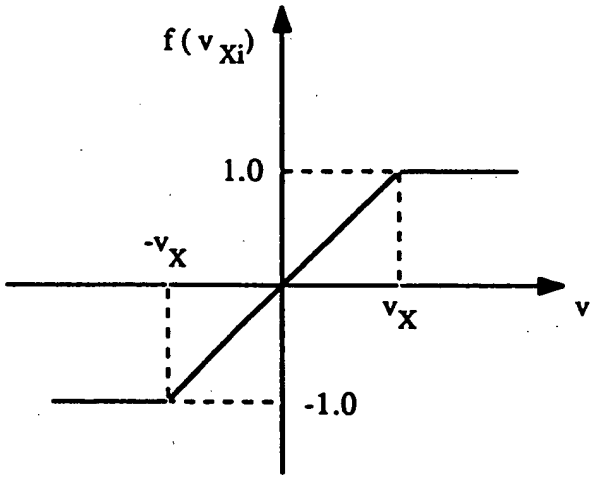

Figure 5. Velocity dependent tire scrub force function.

Energy based rollover stability criteria

In order to analytically investigate the influence of design parameters on a vehicle's rollover stability, decisions must be made regarding the criteria which will be used to quantitatively measure vehicle rollover stability. One widely used rollover stability criteria known as the Static Rollover Stability Factor (SRSF) is defined:

$$SRSF = \frac{\text{Track Width}}{2\ \text{Height}_{cg}} \qquad (6)$$

As shown above, the SRSF is a function of two easily measured vehicle parameters and, as the name implies, is a purely static measure of rollover stability. Because of its simplicity, the SRSF cannot be used to determine the influ-

ence of vehicle design parameters on the dynamic rollover behavior and has mainly been used in statistical studies which attempt to find correlations between SRSF and rollover propensity.

Vehicle rollover is essentially a problem associated with stability. In a rollover situation, a vehicle which generates small roll angles will return to a four wheel stance and is considered stable, however at larger roll angles the vehicle can tip over and is considered unstable. Classical stability theory states that the stability of a system's equilibrium position can be investigated based on the change of the system's potential energy caused by small perturbations of its stated variables. If this change is positive then the system is stable, if negative then the system is unstable. For example, when a vehicle has a roll angle of zero an increase in the roll angle raises its center of gravity position, thus increasing the potential energy of the system, which indicates that the initial position is stable. However, when a vehicle's roll angle equals the static tip over angle then increasing the roll angle will lower the center of gravity position and decreases the system's gravitational potential energy, making the system unstable. The example illustrated above refers to stability of an equilibrium position and could be extended to the more general case of stability of motion. However, this would necessitate investigation into complex and difficult issues related to dynamic analysis (Nalecz (19), (20)). While it is not always practical to perform a classical stability analysis on a complex, non-linear dynamic model it is possible to gain useful information on vehicle response and stability by examining the time history of the vehicle's kinetic and potential energies.

In a majority of tripped rollover accidents, a vehicle's kinetic energy before impact with the tripping obstacle is largely translational. As a result of impact a portion of this translational energy is converted into rotational kinetic energy. If the vechicle gains enough rotational kinetic energy it will roll past its static tip over angle, which represents an unstable equilibrium position. At this point gravitational force acting on the vehicle begins to exert a destabilizing influence, rather than stabilizing, and will pull the vehicle over.

The concept of Rollover Prevention Energy Reserve (RPER) was first introduced by Nalecz et al. (18) and was used as a measure of vehicle rollover stability in the sensitivity analysis of a tripped rollover model. This energy based stability measure examines the difference between the potential energy required to bring the vehicle to the static tip over position and the rotational kinetic energy of the vehicle created as a result of vehicle impact with the curb. If the vehicle has a sufficient amount of rotational kinetic energy to raise the vehicle to its static tip over position and overcome any energy dissipation which might reduce rotational kinetic energy then RPER will become negative, and rollover will occur. RPER is dependent on both static factors such as track width and center of gravity height, and is also dependent on the dynamic response of the vehicle. This makes the time history of RPER dependent on vehicle and environmental parameters as well as the initial conditions of the tripped rollover test. The utilization of RPER in analysis enables determination of the influence of all vehicle design and environmental characteristics on vehicle rollover propensity using a time varying measure of dynamic stability.

During the development of the ITRS the first RPER function (described in (18)) was refined to account for the change in the elastic potential energy of the suspension system and tires as well as to include the effect of suspension crush on the center of gravity position at the static tip over angle. This new measure of RPER was designated RPER3 and is described in (27).

Sensitivity analysis

A vehicle's dynamic system and subsystems (suspensions, brakes, and steering for example) are comprised of many elements whose characteristics directly or indirectly affect its dynamic response. Understanding how design characteristics affect a vehicle's dynamic response is a fundamental step in the design process. Unfortunately, the influence of system parameters on a vehicle's response in a particular maneuver is not always obvious. Sensitivity methods can be used to determine the influence of any vehicle design parameter on its dynamic response, making them very useful in the analysis and synthesis of a complex mechanical system (23–26).

There are various types of sensitivity measures which can be used to investigate the influence of design parameters on vehicle response. These include first order standard, first order percentage, first order logarithmic, and second order standard sensitivity functions (26).

The first order standard sensitivity function is equal to the partial derivative of a system variable taken with respect to a particular system parameter and is useful for determining the influence of a single design parameter on a particular system variable. The first order percentage sensitivity function is calculated by finding the variable change associated with a parameter change of some user specified percentage. Percentage sensitivity functions are useful for comparing the influence of several parameters on a particular system variable. For example, if a designer wished to investigate whether a 2% increase in track width would influence the vehicle's roll angle more than a 2% reduction in center of gravity height then percentage sensitivity could be used. The first order logarithmic sensitivity function is determined by multiplying the first order standard sensitivity function by the parameter value and dividing this product by the variable value. Logarithmic sensitivity functions are dimensionless, making them useful when comparing and ranking the influence of various parameters on system variables. Second order sensitivity functions are determined by calculating the s cond partial derivative of a system variable with respect to a system parameter. Second order sensitivity functi ns can be used to gain additi nal insight into sensitivity results when two or more parameters exhibit

similar first order sensitivity. Table 1 summarizes each sensitivity function.

Table 1. Summary of different sensitivity functi ns.

Sensitivity Type	Analytical Expression	Numerical Expression	Units
1st Order Standard	$\frac{\partial V}{\partial P}$	$\frac{\Delta V}{\Delta P}$	$\frac{V}{P}$
1st Order Percentage	$\frac{\delta V}{\delta P}\delta P$	ΔV	V
1st Order Logarithmic	$\frac{\partial V}{\partial P}\frac{P}{V}$	$\frac{\Delta V}{\Delta P}\frac{P}{V}$	None
2nd Order Standard	$\frac{\partial^2 V}{\partial P^2}$	$\frac{\Delta\left(\frac{\Delta V}{\Delta P}\right)}{\Delta P}$	$\frac{V}{P^2}$

ITRS results

The initial conditions which must be supplied to the ITRS simulation include the vehicle heading angle measured relative to the curb, the initial distance of the vehicle from the curb (measured from the front right tire), and initial velocity of the vehicle center of mass (figure 6).

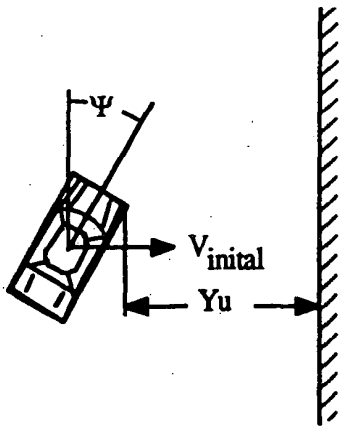

Figure 6. Initial conditions used in intermediate tripped rollover simulation.

The time histories of RPER obtained from the ITRS simulation using data typical of a full size passenger vehicle are illustrated in figures 7 and 8. Figure 7 shows the RPER of a vehicle initially located 7.5 feet from the curb (Yu = 7.5 feet) and parallel to the curb ($\psi = 0$). These initial conditions produced simultaneous front and rear wheel contact with the curb. RPER was computed using initial velocity values of 17, 20, 22.13, 25 and 27 ft/s. In the 17 ft/s case the vehicle came to a stop before reaching the curb and vehicle impact occured in all cases with initial speeds higher than 47 ft/s. The instant of vehicle impact with the curb can be identified on each curve at the point where RPER begins to decrease. The initial velocity of 23.13 ft/s was found to be the threshold speed for tripped rollover in simultaneous impact cases. For initial speeds smaller than 23.13 ft/s vehicle rollover did not occur and the RPER curves for these speeds always remained positive. However, the results obtained using initial velocities greater than or equal t 23.13 ft/s resulted in rollover and the RPER reached negative values. At 23.13 ft/s the minimum value of RPER is only slightly negative, but as the speed increases the minimum values of RPER become strongly negative. These results indicate that RPER is a very useful dynamic function for assessing the rollover potential of a vehicle in a simultaneous tripped rollover situation.

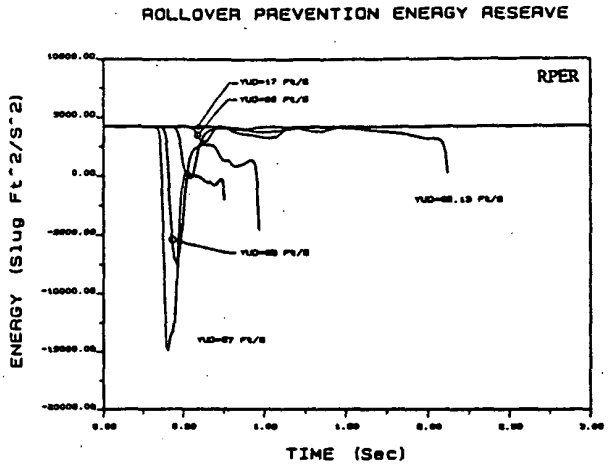

Figure 7. RPER of ITRS in simultaneous impact case (Ψ=0 degrees).

The curves shown in figure 8 illustrate the RPER of a vehicle which is initially located 7.5 feet away from the curb (Yu = 7.5 ft) and has an initial yaw angle $\psi = 25$ degrees. The values of RPER were computed using initial velocities of 17, 20, 23.73, 25 and 27 ft/s. As before, the vehicle came to a stop prior to impact with the curb in the 17 ft/s case. Rollover occurred in the 23.73, 25 and 27 ft/s cases, however, the 20 ft/s case did not result in rollover. The initial velocity of 23.73 ft/s was found to be the rollover threshold speed for the initial conditions of this oblique impact. In the oblique impact the minimum value of RPER at the rollover threshold speed falls below the minimum value of RPER which occurs in the simultaneous impact case. This is because when the vehicle strikes the curb at a positive oblique angle the front wheels of the vehicle strike the curb first, the vehicle then yaws until the rear wheels strike the curb, and then the vehicle rolls over. A palpable amount of energy is dissipated during the time period between the front and rear wheel impacts and the vehicle must possess enough excess kinetic energy to overcome this dissipation if a rollover is to occur.

The sensitivity methods developed by the University of Missouri-Columbia (Nalecz and Bindemann (21, 22)) have been utilized to determine the influence of various vehicle design parameters on the time history of a vehicle's RPER in tripped rollover maneuvers. The sample sensitivity results presented in figures 9–12 have been obtained in simultaneous impact at the r llover threshold speed of 22.13 ft/s. The percentage sensitivity functions which have been chosen for analysis represent the variabl change caused by a 1 percent parameter change and can be interpreted in the following manner. If the percentage sensitivity function is positive then this indicates that an increase the parameter

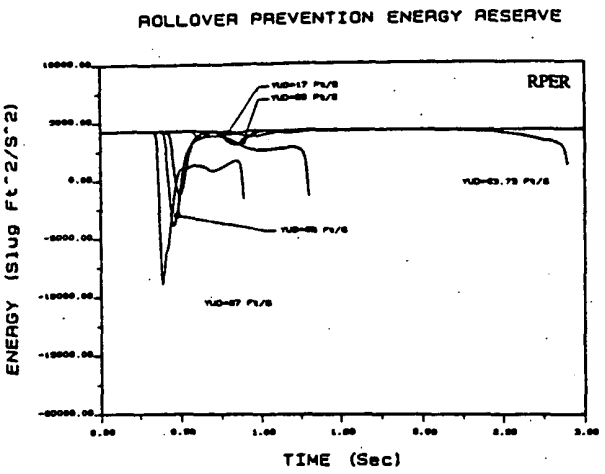

Figure 8. RPER of ITRS in oblique impact case (Ψ=25 degrees).

value results in an increase in the variable, which in this case, is RPER. If the sensitivity function is negative this indicates that an increase of the parameter value will decrease the variable value.

The time period on these sensitivity graphs which provides the greatest amount of information on how parameter changes can influence the rollover propensity of a vehicle begins at the start of the curve (t = 0) and ends at the point of rollover initiation. This paper designates the point of rollover initiation as the instant when RPER becomes negative.

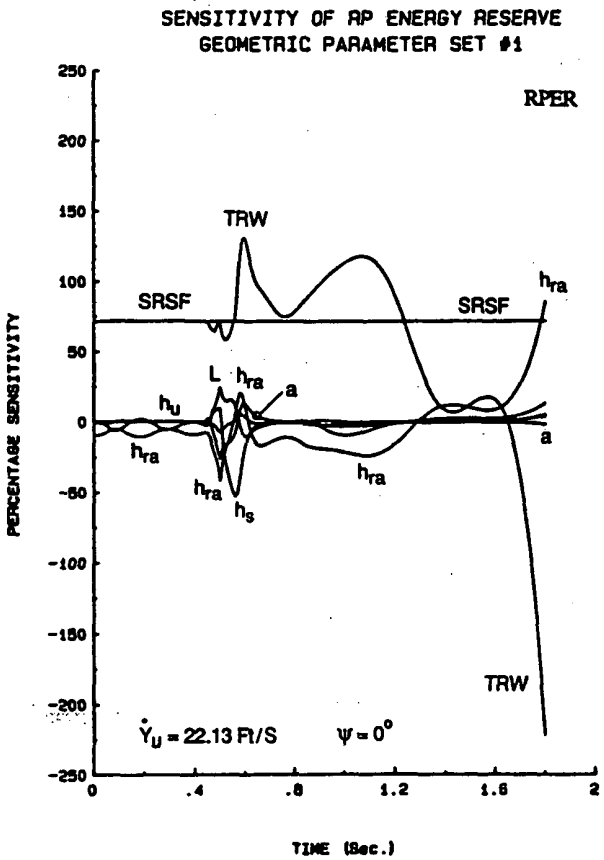

Figure 9. Sensitivity of ITRS RPER for geometrical parameters set No. 1.

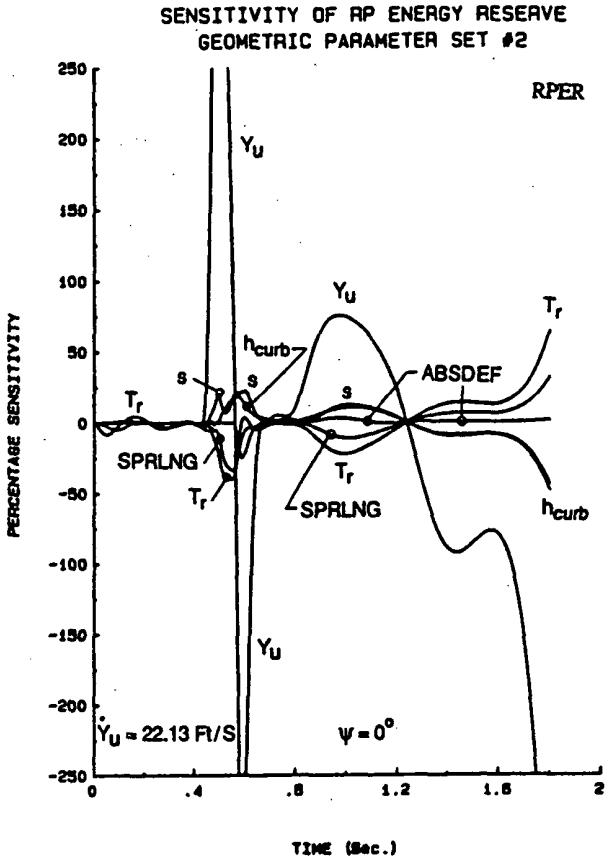

Figure 10. Sensitivity of ITRS RPER for geometrical parameter set No. 2.

For the initial conditions used to generate the sensitivity functions shown in figures 9–12 the point of rollover initiation occurs at approximately 0.58 seconds. The primary reason for limiting the analysis to this time period is this; what happens to the vehicle in this time period determines whether or not rollover will occur.

Figures 9 and 10 show the influence of geometric parameters on RPER. The most important parameters in figure 9 are the track width TRW and the static stability rollover factor SRSF. Because the SRSF is a purely static measure of rollover stability its sensitivity function remains constant and does not change with time. Track width TRW, however, does exert a dynamic influence on the system and its sensitivity function changes with time. The results show that vehicle rollover stability can be increased by increasing the vehicle track width (and therefore its static stability rollover factor). The influence of other parameters in figure 9 are much smaller than those of TRW and SRSF.

Figure 10 shows that the initial distance from the curb Yu has a very large influence on RPER and that increasing Yu results in a very large transient increase of RPER. The reason for positive values of sensitivity functions of Yu is that a vehicl which is farther away from the curb must slide a longer distance before impact, and therefore it will dissipate a greater amount of its translational kinetic energy before impact and will strike the curb at a lower speed than a vehicle which begins its m tion closer to the curb. However,

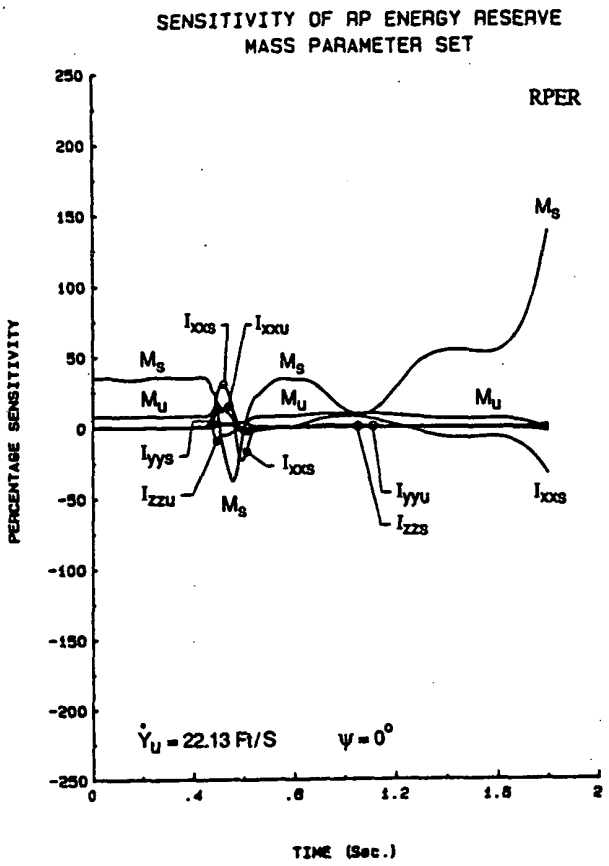

Figure 11. Sensitivity of ITRS RPER for mass/inertia parameter set.

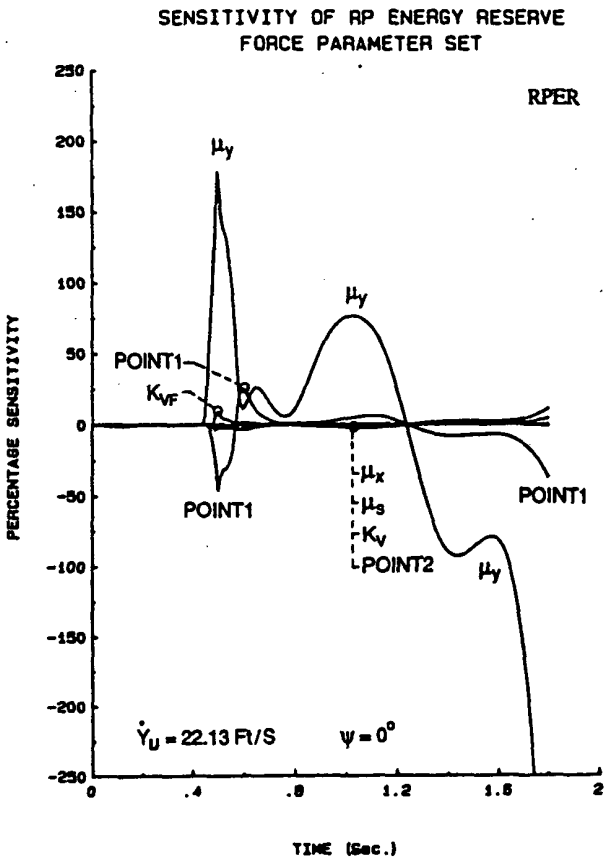

Figure 12. Sensitivity of ITRS RPER for force parameter set.

the transient behavior (and relatively large values) of the sensitivity function increase is caused by the nature of the sensitivity methods used in this analysis (see Nalecz and Bindemann (21, 22)). Other influential parameters on figure 10 are the undeformed suspension spring length SPRLGN and tire radius T_r. The figure indicates that increasing either of these parameters will decrease RPER, which is very reasonable since increasing T_r or SPRLGN parameters has a secondary effect of raising the vehicle center of gravity.

Figure 11 illustrates the influence of vehicle mass and inertia parameters on RPER. The figure shows that increasing the sprung mass initially increases the vehicle's RPER, however, after impact the sprung mass exerts a negative influence on RPER. This is because after impact the inertia force of the vehicle tends to rotate the vehicle about the curb, and therefore a larger sprung mass will produce a larger inertia force as a result of impact. The increases of the roll moments of inertia of sprung and unsprung masses I_{xxs} and I_{xxu} produced increases of vehicle RPER during impact, which was expected, since the roll moments of inertia oppose the roll acceleration of the vehicle.

The influence of impact and force parameters on vehicle RPER is illustrated in figure 12. As seen in this figure the pavement friction coefficient μ_y exerts a str ng p sitive influenc on RPER. This is l gical since the majority f kinetic energy which is l st pri r to impact with the curb is dissipated by the frictional forces generated by the tires. A higher friction coefficient will produce higher friction forces and the loss of additional kinetic energy prior to impact, resulting in lower impact speeds. Figure 12 also shows that increasing the elastic region of the impact force deformation curve (Point 1, figure 4) will decrease vehicle RPER. Because plastic deformation during impact will dissipate a portion of the vehicle's kinetic energy plastic deformation helps to reduce the risk of rollover and the onset of plastic deformation can be hastened by reducing the size of the elastic deformation region.

Intermediate Maneuver Induced Rollover Simulation

In the past, there has been a considerable amount of debate and controversy surrounding the phenomenon of maneuvered induced rollover. These are rollover accidents which typically occur on smooth pavement and are initiated by driver steering and braking inputs, rather than an excursion into a roadside feature. While maneuver induced rollover accidents occur infrequently in comparison to tripped rollover accidents, it is justifiably argued that a vehicle should n t rollover as a result of steering and braking inputs which might occur in a collision av idance situation. Much of this c ntroversy centers around off-road utility vehicles and light pick-up trucks. Critics of these vehicles claim that the high ground clearances associated with these vehicles

result in a high center of gravity, and increase their rollover propensity.

The Intermediate Maneuver Induced Rollover Simulation (IMIRS) developed by Nalecz (28) can be used to investigate vehicle maneuver induced rollover as well as limit handling maneuvers. The IMIRS represents an extension of the Lateral Weight Transfer Simulation (LWTS) described in (29). Like the ITRS the IMIRS utilizes a vehicle model of intermediate detail, which requires a modest amount of vehicle data and computation time.

IMIRS model description

The IMIRS simulation utilizes two coupled vehicle dynamic models to simulate handling and rollover behavior; an illustration of each model is given in figures 13 and 14. The vehicle handling model has 3 degrees of freedom, while the rollover model is a 5 degree of freedom model.

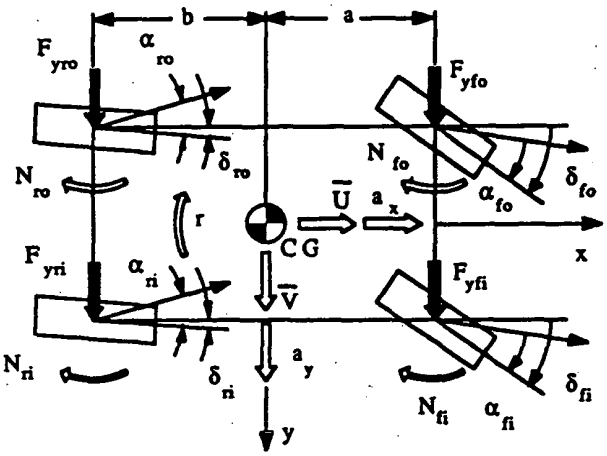

Figure 13. IMIRS handling model.

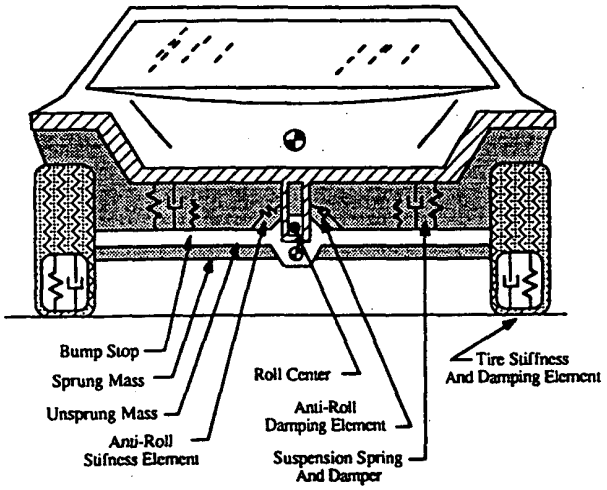

Figure 14. IMIRS rollover model.

The generalized velocities used in the handling model are forward velocity U, lateral velocity V and yaw rate r. The equations of motion employed in the vehicle handling model have been obtained from the Newt n-Euler formulation:

The external forces and moments which act on the IMIRS

$$\Sigma F_x = m (\dot{U} - r V)$$

$$\Sigma F_y = m (\dot{V} + r U) \qquad (7)$$

$$\Sigma M_z = Iz \dot{r}$$

handling model are those generated by pneumatic tires, gravitational and aerodynamic effects. A non-linear tire model based on the non-dimensional slip angle approach was employed in the simulation. The tire model determines the side force, braking force, and aligning moment generated by a tire in combined cornering and braking maneuvers based on the conditions of normal load, longitudinal slip, slip angle, and camber angle which are imposed on the tire. Example plots of side force versus slip angle and braking force versus slip ratio are shown in figures 15 and 16.

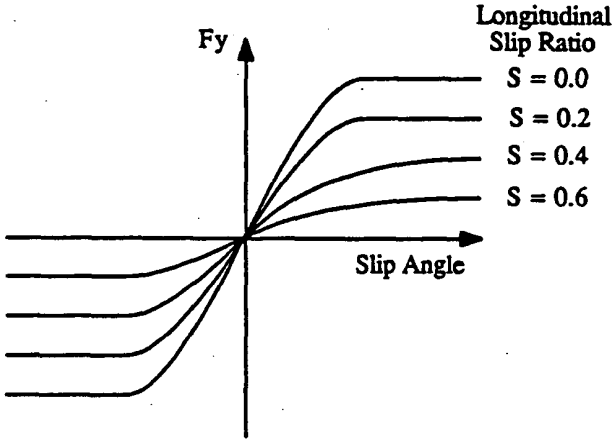

Figure 15. Tire side force versus slip angle in IMIRS simulation.

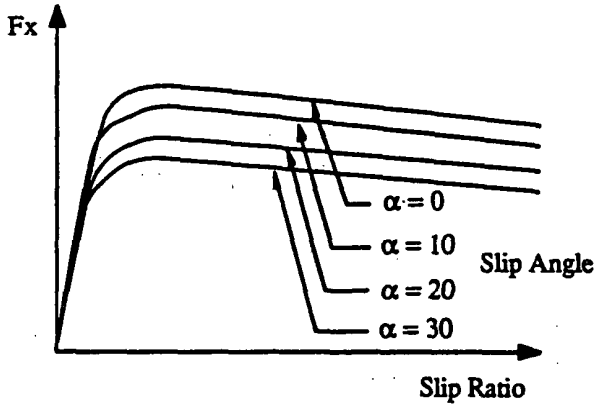

Figure 16. Tire braking force versus slip ratio in IMIRS simulation.

If the applied brake torque exceeds the frictional torque produced by the force generated at the tire/pavement interface then the tire is assumed to become locked and the sliding frictional force is assumed to act in a direction opposite the tire's direction f motion. If the applied thrust torque exceeds the tires traction ability then the tire is assumed to begin spinning and the tire thrust f rce acts in the direction

of the wheel plane. The friction ellipse is used to determine the tire limits of adhesion in all directions and is shown in figure 17.

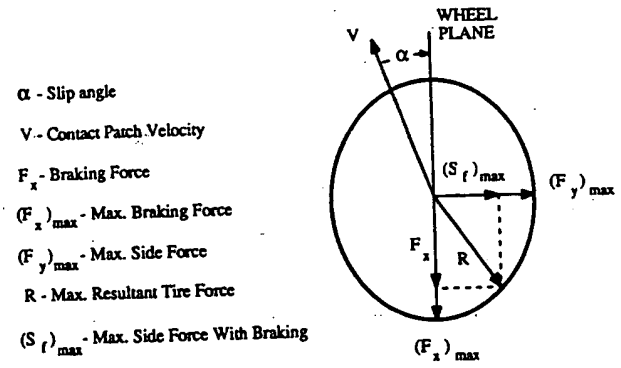

Figure 17. Friction ellipse in combined cornering and braking conditions.

The size and aspect ratio of the ellipse is dependent on the peak braking and cornering friction coefficients, pavement conditions, and tire normal load. The IMIRS tire model uses Calspan tire data to determine the following tire characteristics:

- Cornering Stiffness
- Camber Stiffness
- Peak Cornering Friction Coefficient
- Peak Braking Friction Coefficient
- Sliding Friction Coefficient
- Slip Ratio at Peak Braking
- Aligning Moment

These characteristics are computed as functions of tire normal and side loads. The aerodynamic side force together with aerodynamic yaw damping are also included in the model.

In order to investigate untripped vehicle rollover behavior, a vehicle rollover model has been added to the IMIRS to work in conjunction with the handling model. It is a planar model and consists of two masses, sprung and unsprung, which are connected through the various elements of the suspension system. The rollover model is coupled to the vehicle handling model through the external forces which are applied to the planar model. These forces include the side forces generated by the tires, the inertial forces acting on the sprung and unsprung masses, and gravity. The degrees of freedom used in the IMIRS rollover model include:

ϕ_u—Roll angle of the unsprung mass

y_u—Lateral displacement of the unsprung mass center of gravity

z_u—Vertical location of the unsprung mass center of gravity

ϕ_s—Roll angle of the sprung mass relative to the unsprung mass

z_s—Heave of sprung mass relative to the unsprung mass

The equations of motion of the rollover were derived using the Lagrangian formulation (28).

The suspension system used in the rollover model is similar to that used in the ITRS and is illustrated in figure 14. The sprung mass motion is constrained using a pin which slides in a vertical slot in the unsprung mass. Two linearly elastic springs and viscous dampers support the sprung mass. Bump stops limit the relative motion of the sprung mass in roll and heave. These bump stops are modelled using non-linear, hardening springs which become infinitely stiff if compressed to zero length. The front and rear tires are combined at the left and right sides of the vehicle and are modelled using a linearly elastic spring placed in parallel with a viscous damping element.

IMIRS rollover prevention energy reserve

Rollover prevention energy reserve was used in the ITRS simulation as a dynamic measure of vehicle stability in tripped rollovers. The concept of RPER has also been applied to the IMIRS to assess vehicle stability in maneuver induced rollover situations. The formulation of RPER used in the IMIRS differs slightly from that used in the ITRS because of the differences between the two maneuvers. The IMIRS determines RPER by subtracting the kinetic energy of vehicle rolling motion, obtained from the Lagrangian formulation of the rollover model, from the amount of potential energy required to raise the vehicle center of gravity from its instantaneous position to the static tip over position. This measure of RPER is designated $RPER_a$.

Results obtained from IMIRS

The IMIRS was used to simulate a J-turn maneuver using vehicle data typical of a small off-road utility vehicle. This maneuver simulates a vehicle being driven in a straight line at 58.67 ft/s (40 miles per hour) and given a ramp steering wheel input of 240 degrees in 0.5 seconds. The steering wheel was then held stationary. The pavement conditi ns used in the simulation had a moderately high coefficient of friction (SN = 110). A high coefficient of friction was chosen so that the vehicle could generate a value of lateral acceleration sufficient to cause rollover. If the road surface had a low coefficient of friction, such as that of wet pavement, then the vehicle would tend to skid or spin out rather than rollover. The roll angle of the unsprung mass as well as the roll angle of the sprung mass measured relative to the unsprung mass are shown in figure 18.

The time history of $RPER_a$ obtained in the J-turn maneuver is presented in figure 19. The shape of this RPER curve is qualitatively different from the characteristic shape produced in the tripped rollover cases. These dissimilarities are caused by fundamental differences between tripped and maneuver induced rollover behavior. RPER in its most basic form represents the change in potential energy required to raise the vehicle center of gravity to the static tip over positi n minus the rotational kinetic en rgy of the vehicle. In the case of tripped roll ver the rotational kinetic energy of the vehicle reaches a maximum value shortly after impact with the curb and then decreases as the vehicles rotate to the static tip over angle. In maneuver induced rollover acci-

dents the rotational kinetic energy of the vehicle tends to increase continuously.

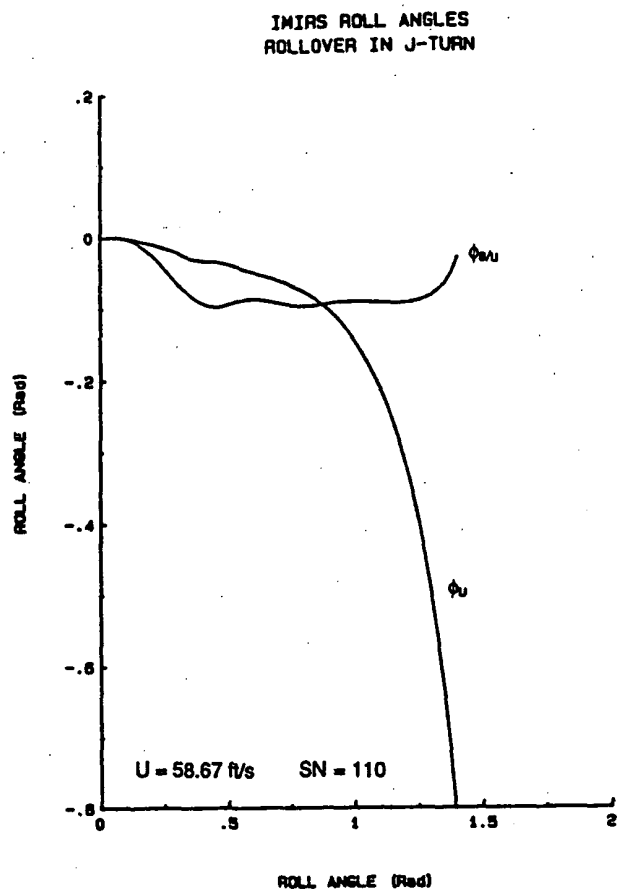

Figure 18. IMIRS vehicle roll angle in J-turn rollover.

The sensitivity of vehicle $RPER_a$ to selected parameter groups in the 40 mile per hour J-turn maneuver has been performed utilizing percentage sensitivity functions. The influence of two groups of vehicle geometrical parameters on $RPER_a$ is shown in figures 20 and 21. Figure 20 indicates that an increase of the sprung mass center of gravity height decreases vehicle $RPER_a$, while an increase in the front and rear track widths increases $RPER_a$.The influence of geometrical parameter set #2 is shown in figure 21 from which it is seen that $RPER_a$ can be raised by increasing spring track widths. Changes in front and rear roll center heights RC_f and RC_r, static suspension spring length SPRLNG, and undeformed bump stop length BSLNG appear to have very little effect on $RPER_a$ in the J-turn maneuver induced rollover. The most influential geometrical parameters appear to be, in order of importance, sprung mass center of gravity height, front and rear track width, suspension spring track width, the distance from the front axle to the vehicle c.g. a, and the unsprung mass center f gravity heights H_{UF} and H_{UR}.

The influence of vehicle mass/inertia parameters on $RPER_a$ is present d in figure 22. Th results show that the sprung mass initially has a beneficial effect, however, when the vehicle beings to roll an increase in the sprung mass

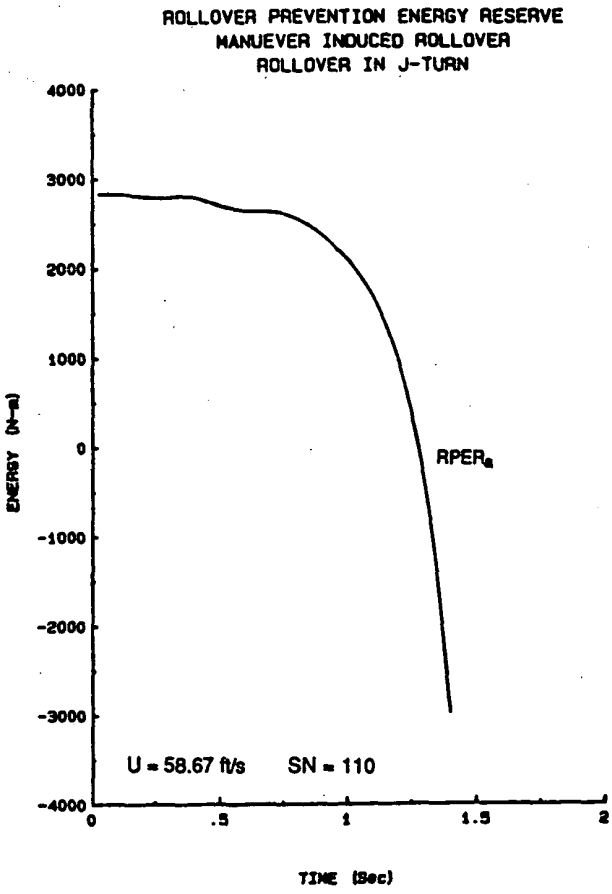

Figure 19. IMIRS vehicle $RPER_a$ in J-turn rollover.

reduces $RPER_a$. Increases in the unsprung masses (M_{uf} and M_{ur}) and yaw moment of inertia I_{zz} seem to have a positive influence on $RPER_a$, however, an increase of the sprung mass roll moment of inertia I_{xxs} tends to reduce $RPER_a$. This seems to contradict the results obtained from the sensitivity analysis of the ITRS where an increase in the vehicle roll moment of inertia raised vehicle RPER. One reason for this difference is that in the maneuver induced rollover the sprung mass roll acceleration changes signs as the sprung mass rolls to the outside and is then stopped by the suspension elements which oppose this motion. Since inertia tends to oppose acceleration it may exert a negative influence in a maneuver induced rollover. The figure also shows that shifting the vehicle weight distribution toward the rear of the vehicle increases $RPER_a$, in agreement with the sensitivity of parameter as shown on figure 20.

The sensitivity of $RPER_a$ to changes in the stiffness parameters is illustrated in figure 23. The figure shows that $RPER_a$ can be increased by increasing the stiffness of the suspension springs and tires K_1 and K_z and by shifting the vehicle roll stiffness distribution KR_{dist} toward the front of the vehicle. The stiffness of the bump stops K_2 as well as the auxiliary roll stiffness contribution from anti-roll bars K_{rf} and K_{rr} had little influence on vehicle $RPER_a$ in the roll ver induced by the J-turn.

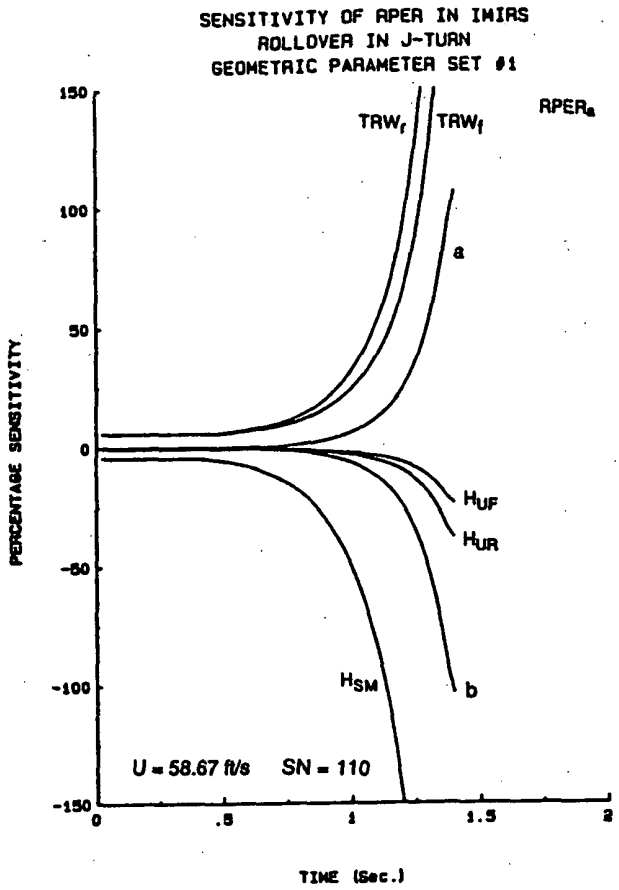

Figure 20. Sensitivity of IMIRS RPER$_a$ for geometrical parameter set No. 1.

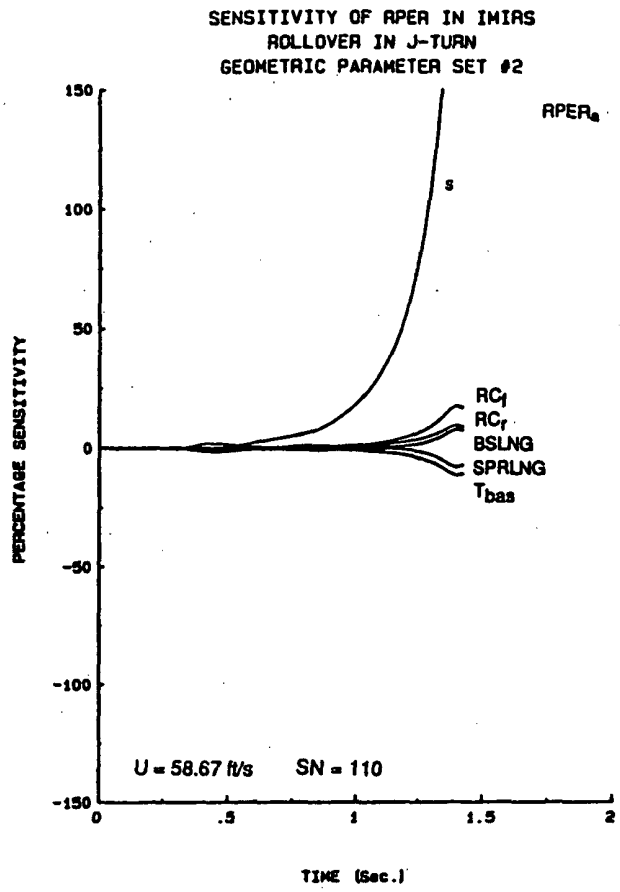

Figure 21. Sensitivity of IMIRS RPER$_a$ for geometri al parameter set No. 2.

An Overview of the Advanced Vehicle Rollover Model (AVRM)

The University of Missouri-Columbia is currently in the process of developing a complex simulating program (30) which will be capable of providing detailed analysis into all of the most common types of rollover accidents. The Advanced Vehicle Rollover Simulation (AVRM) will be able to simulate maneuver induced rollovers, as well as rollovers caused by vehicle excursions into roadside features such as curbs, soft soil, and embankments. The vehicle model assumed in the AVRM simulation has 14 degrees of freedom. The sprung mass has 6 degrees of freedom, three translational and three rotational. Each suspension system has 2 degrees of freedom and each wheel has a rotational degree of freedom. All phases of various rollover events will be simulated including pre-rollover motion, rollover initiation, rollover and post impact motion. The simulation will be able to provide an estimate of rollover impacts severity using a sprung mass/ground impact model.

The AVRM will be capable f simulating virtually any type f independent suspension system through an equivalent swing arm suspension model (figure 24). The pivot point of each swing arm is placed at the wheel's instant center in static conditions and this location is determined based on a kinematic analysis of the suspension system. Dependent suspension systems are modelled using a beam axle representation (figure 25). The beam axle is assumed to pivot about the static roll center of the suspension and can translate in a vertical direction relative to the sprung mass. The suspension springs have non-linear stiffness characteristics which are computed using polynomial functions of displacement with coefficients which are determined experimentally. The damping rate of each shock absorber is a quadratic function of the damper's rate of displacement. Both independent and dependent suspension systems have elastic and viccous damping anti-roll elements. Both types of suspensions, independent and dependent, can be employed in any combination at the front and rear of the vehicle.

The frictional tire model used in the AVRM is based on the non-dimensional slip angle approach and utilizes a dual friction ellipse concept to determine the limits of adhesion in different directions under combined conditions of cornering and braking r thrust. This model includes modifications to account for the large values of camber angles, as well as overload conditions which can occur during tire impacts with roadside features such as a curb. Several discontinuities which existed in the previous

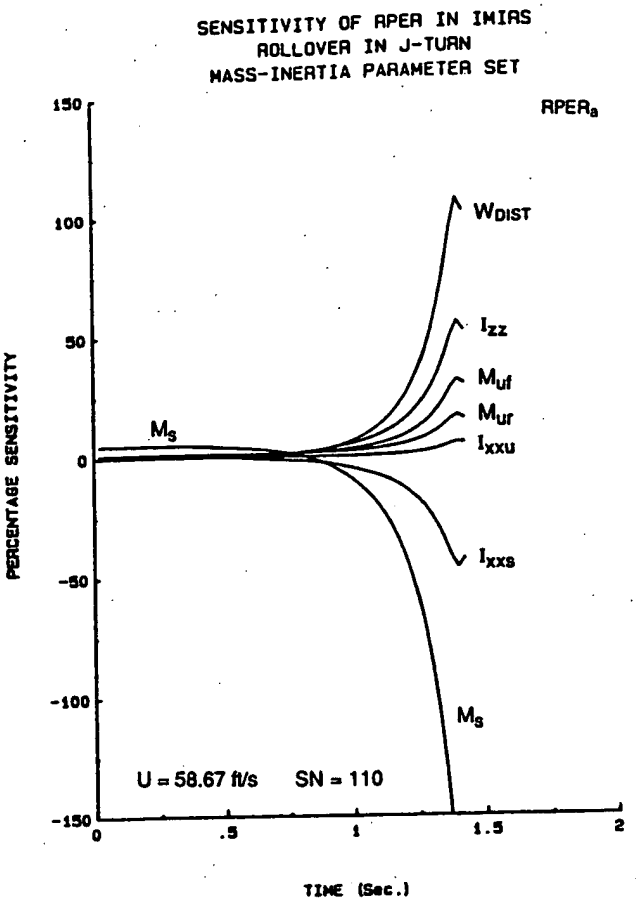

Figure 22. Sensitivity of IMIRS RPER$_a$ for mass/inertia parameter set.

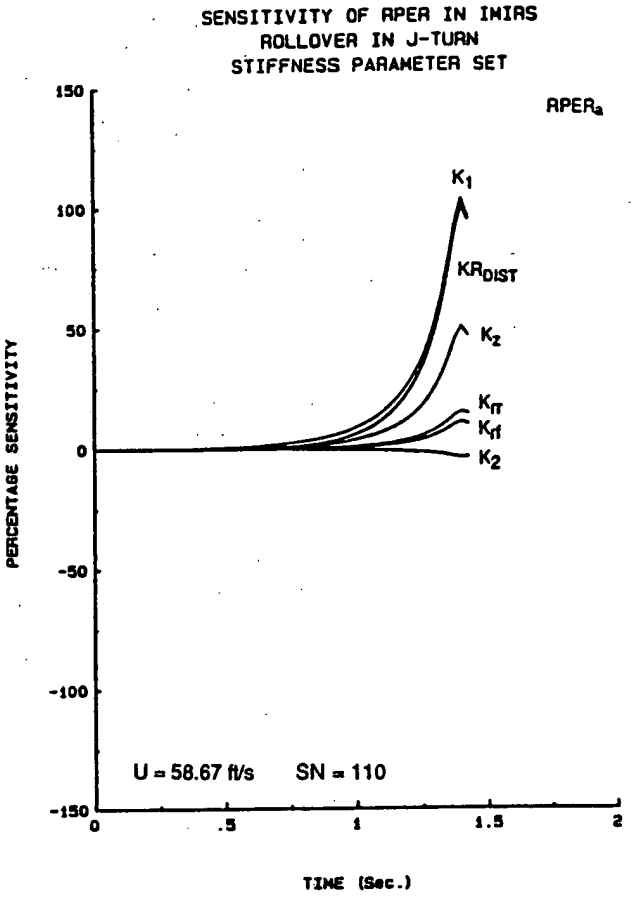

Figure 23. Sensitivity of IMIRS RPER$_a$ for stiffness paramet r set.

version of the tire frictional model under conditions of combined cornering and braking have been eliminated through the development of a dual friction ellipse representation. Figure 26 and 27 show examples of side force vs. slip angle at various camber angles in both free rolling and heavy braking conditions.

The forces and moments generated during vehicle impact with roadside features are computed based on the three dimensional state of the tire caused by interference with the terrain profile. The tire impact model is illustrated in figures 28 and 29. Figure 28 shows the three dimensional representation of the tire impacting with a curb at an oblique angle. The impact model consists of numerous springs which have been specially arranged to ensure that the generated impact reactions are adequate in various vehicle maneuvers including those which produce excessive camber angles and overloads. A radial cross section detailing the spring locations and orientations used in the tire model can be seen in figure 29. The deformation of each spring is determined based on the wheel's orientation relative to the terrain surface. The forces and moments produced by each elastic element are then totalled to obtain the net reaction f each wheel.

A vehicle/ground impact m del employs 21 node points

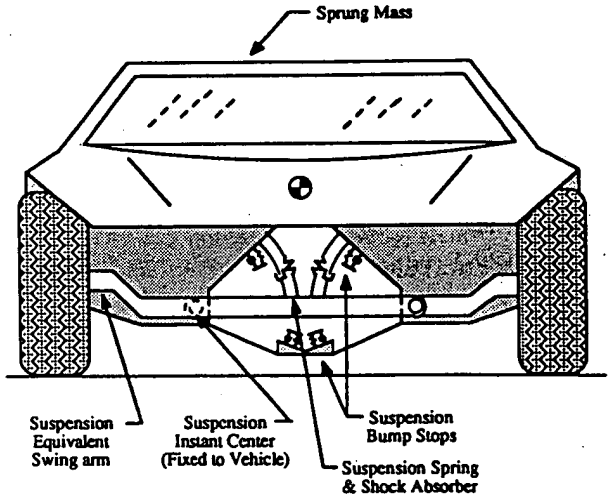

Figure 24. AVRM equivalent swing arm representation f independent suspension.

to generate reactions during sprung mass contact with the ground. The forces produced by each node are based on both the amount and rate of change of deformation. The f rce/ deflection characteristics of each node are similar to those used in the wheel/curb impact m del of the ITRS (figure 4).

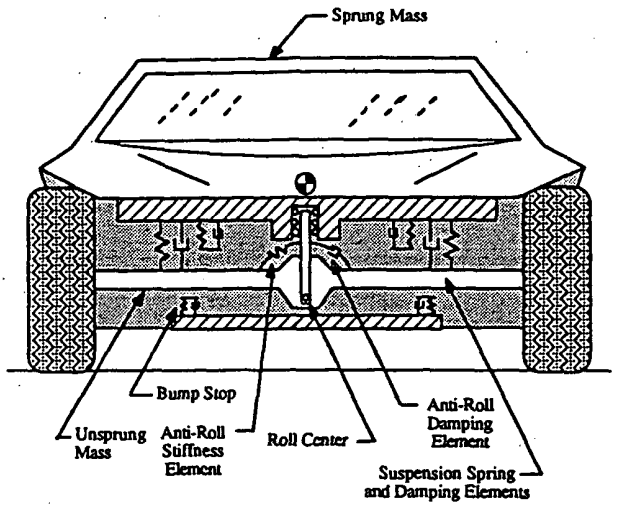

Figure 25. AVRM representation of dependent suspension system.

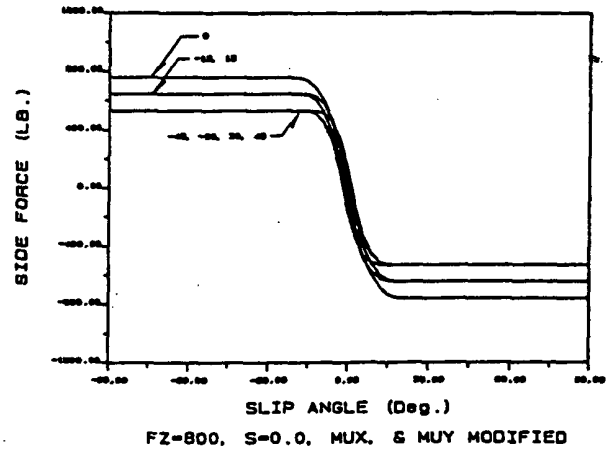

Figure 26. Side force versus slip angle in free rolling conditions at various camber angles.

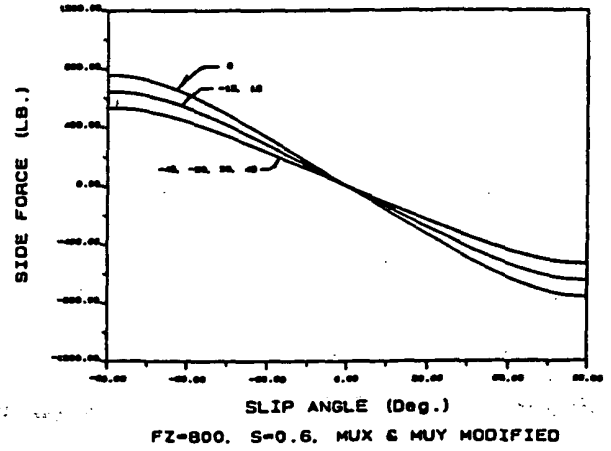

Figure 27. Side force versus slip angle in heavy braking conditions at various chamber angles.

These deformation characteristics account for both elastic and plastic deformation at each node and can be used to

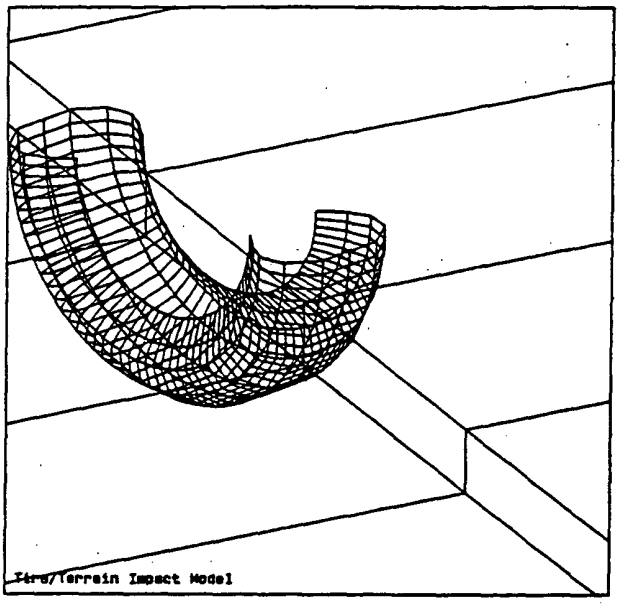

Figure 28. AVRM tire terrain impact model.

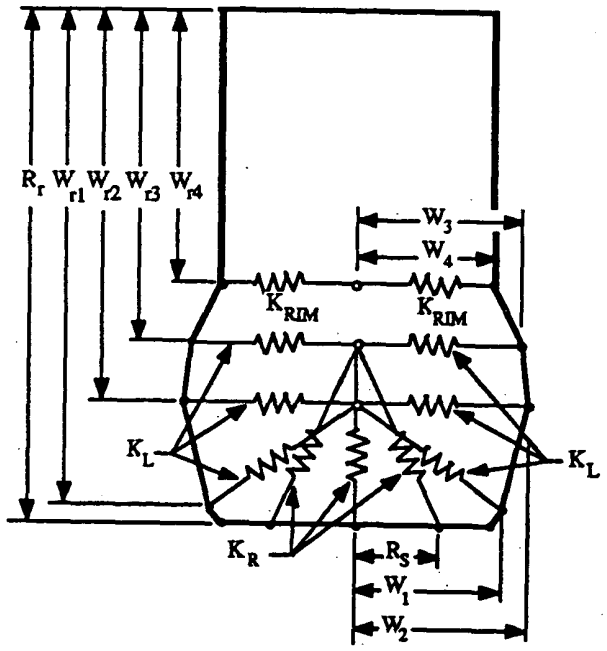

Figure 29. Cross section of tire impact model.

estimate the severity of the rollover event. The fricti nal scrub force generated by each node are calculated as a function of the normal reaction and sliding velocity of each node. Examples obtained during testing of the sprung mass ground impact model are shown in figures 30 and 31.

The equations of motion for the AVRM are derived using the Lagrangian formulation in quasi-coordinates. In addition to sprung and unsprung masses the AVRM model permits inclusion of 6 additional masses which can be used to investigate the effects of various passenger/payload configurations.

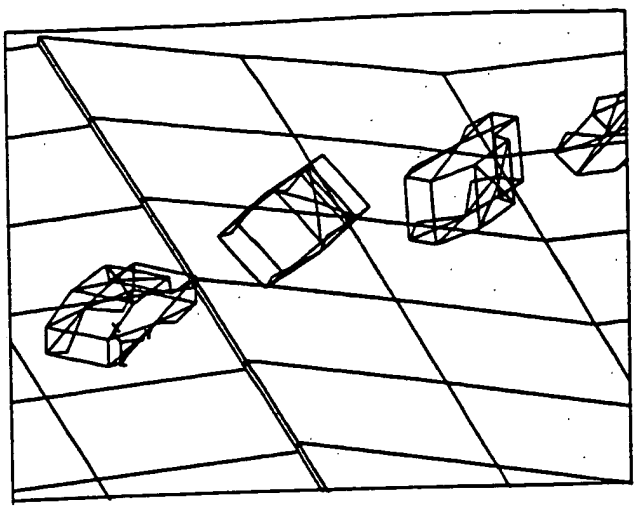

Figure 30. AVRM tripped rollover simulation.

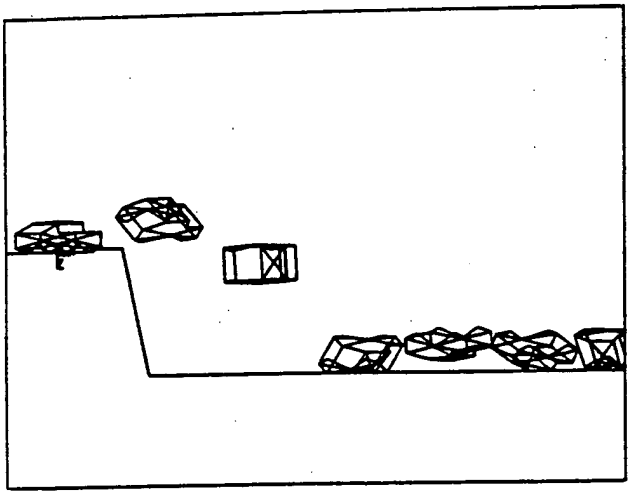

Figure 31. AVRM sprung mass ground impact model test.

Conclusions

The results presented in this paper show that ITRS and IMIRS simulations are very useful for predicting the occurrence of rollover and, when used in conjunction with sensitivity methods, represent powerful tools which can determine the influence of vehicle design parameters on dynamic rollover behavior.

The concept of Rollover Prevention Energy Reserve is a reliable indicator of dynamic rollover stability. The results reveal that the minimum value of RPER approaches zero at the threshold of rollover and if this minimum falls below zero then vehicle rollover will occur. Finding the effects of parameter variations on RPER using sensitivity methods represents a practical, productive approach when investigating the influence of vehicle and environmental parameters on rollover propensity. The vast majority of results obtained using this approach have agreed with statistical observations and prevailing opinion.

A great deal of useful experience was gained during the development of the ITRS and IMIRS simulations and has proved m st useful while developing the AVRM model. Preliminary results obtained while testing AVRM subsystem models are quite promising and indicate that it will be a very useful tool for investigating of all types of rollover accidents.

References

(1) Maryland State Police, "Maryland Rollover Data File," Accident Data Collected for NHTSA R&D, U.S. DOT, Washington D.C., 1988.

(2) National Accident Sampling System (NASS) 1985 Data Base, National Center for Statistics and Analysis, NHTSA, U.S. DOT, Washington D.C., 1985.

(3) Edwards, M.L., "A Database for Crash Avoidance Research," SAE Special Publication NO. 699, 1987.

(4) NHTSA—U.S. DOT, "Fatal Accident Reporting System 1986," A Review of Information on Fatal Traffic Accidents in the United States in 1986, Washington D.C., 1986.

(5) Jones, I.S., "Vehicle Stability Related to Frequency of Overturning for Different Models of Cars," Proc. Australian Road Research Board, Vol. 7, Part 5, 1974.

(6) Snyder, R.C., et al., "On-Road Crash Experience of Utility Vehicles," HSRI, University of Michigan, Report No. UM-HRSI-80-14, February 1980.

(7) Insurance Institute for Highway Safety, "Small Passenger Vehicles a Problem," IIHS Status Report, Vol. 22, No. 2, February 1987.

(8) Griffin, L.I., III, "Probability of Overturn in Single Vehicle Accidents as a Function of Road Type and Passenger Car Curb Weight," Traffic Accident Research and Evaluation Program, Texas Transportation Institute, Texas A&M University System, November 1981.

(9) Griffin, L.I., III, "Probability of Driver Injury in Single Vehicle Collisions with Roadway Appurtenances as a Function of Passenger Car Curb Weight," Texas Transportation Institute, Texas A&M University System, October 1981.

(10) Reinfurt, D.W., et al., "A Comparison of the Crash Experience of Utility Vehicles, Pickup Trucks and Passenger Cars," Highway Safety Research Center, University of North Carolina, September 1981.

(11) Reinfurt, D.W., et al., "A Further Look at Utility Vehicle Rollover," Highway Safety Research Center, University of North Carolina, August 1984.

(12) Malliaris, A.C., et al., "Problems in Crash Avoidance Research," SAE International Congress & Exposition, Detroit, Michigan, SAE Paper No. 830560, 1983.

(13) Habberstad, J.L., Wagner, R.C., Thomas, T.M., "Rollover and Interior Kinematics Test Procedures Revisited," SAE Paper No. 861875, 1986.

(14) Segal, D.J., "Highway Vehicle Object Simulation Model," FHWA—U.S. DOT Final Report No. FHWA-RD-76-162, 1976.

(15) Jones, I.S., "The Mechanics of Rollover as the R sult of Curb Impact," SAE Paper 7650461, 1975.

(16) DeLeys, N.J., Parada, L.O. "Rollover Potential of

Vehicles on Embankments, Sideslopes, and Other Roadside Features," FHWA—U.S. DOT Final Report No. FHWA-RD-86-164, 1986.

(17) Rosenthal, T.J., et al., "User's Guide and Program Description for a Tripped Roll Over Vehicle Simulation," NHTS—U.S. DOT Report No. DOT HS 807140, 1987.

(18) Nalecz, A.G., et al., "Sensitivity Analysis of Vehicle Tripped Rollover Model," NHTSA—U.S. DOT Report No. DOT HS 807 300, July 1988.

(19) Nalecz, A.G., "The Nonholonomic Constraints of a Vehicle on Pneumatic Tires," Vehicle System Dynamics, v. 12, n. 1-3, July 1983, 8th IAVSD Symp on the Dyn of Veh on Roads and Tracks, MIT, Aug. 14-19, 1983.

(20) Nalecz, A.G., "Dynamic Equilibrium of a Motor Car Vehicle Under Action of Oblique Airflow," *Nonlinear Vibration Problems*, Vol. 18, No. 9, pp. 107-145, 1977.

(21) Nalecz, A.G., Bindemann, A.C., "Sensitivity Analysis of Vehicle Design Attributes that Affect Vehicle Response in Critical Accident Situations—Part I: User's Manual," Final Report NHTSA—U.S. DOT No. DOT HS 807229, October 1987.

(22) Nalecz, A.G., Bindemann, A.C., "Sensitivity Analysis of Vehicle Design Attributes that Affect Vehicle Response in Critical Accident Situations—Part II: Technical Report," Final Report NHTSA—U.S. DOT No. DOT HS 807 230, November 1987.

(23) Nalecz, A.G., Wicher, J., "Design Sensitivity Analysis of Mechanical Systems in Frequency Domain," *Journal of Sound and Vibration*, Vol. 120, No. 3, pp. 517-526, 1988.

(24) Wicher, J., Nalecz, A.G., "Second Order Sensitivity Analysis of Lumped Mechanical Systems in the Frequency Domain," *International Journal for Numerical Methods in Engineering*, Vol. 24, No. 12, pp. 2357-2366, 1987.

(25) Nalecz, A.G., "Sensitivity Analysis of Vehicle Design Attributes in Frequency Domain," *International Journal of Vehicle System Dynamics*, Vol. 17, No. 3, pp. 141-163, 1988.

(26) Nalecz, A.G., "Application of Sensitivity Methods to Analysis and Synthesis of Vehicle Dynamic Systems," State of the Art Paper at 11th IAVSD Symp on the Dyn of Veh on Roads and Tracks, Kingston, Canada, August 1989.

(27) Nalecz, A.G., Bare, C., "Development and Application of ITRS," NHTSA—U.S. Department of Transportation, Contract No. DTNH22-87-D27174, Final Report 1989.

(28) Nalecz, A.G., "Intermediate Maneuver Induced Vehicle Rollover Simulation," TSC—U.S. Department of Transportation, Contract No. DTRS57-88-P-82668, Final Report, 1989.

(29) Nalecz, A.G., "Investigation into the Effects of Suspension Design on Stability of Light Vehicles," *SAE Transactions*, Vol. 96, No. 1, Paper No. 870497, 1987.

(30) Nalecz, A.G., et al., "Advanced Dynamic Rollover Model," NHTSA—U.S. Department of Transportation, Contract No. DTNH22-87-D-27174, Final Report 1989.

Real World Rollovers—A Crash Test Procedure and Vehicle Kinematics Evaluation

T. M. Thomas,
N. K. Cooperrider,
S. A. Hammoud,
P. F. Woley,
Failure Analysis Associates, Inc.

Abstract

Until recently, crash tests to study real world rollover accidents have used either snubbed dollies or guided ramps. Neither method accurately represents what occurs during a curb trip rollover accident. This paper discusses a series of rollover tests conducted by Failure Analysis Associates, Inc. (FaAA), in which the test vehicles are slid sideways, released from tow, and tripped by a curb, as could occur in a real accident. Another vehicle was launched from a FMVSS 208 dolly for comparison. The test vehicles contained unrestrained front seat anthropomorphic dummies.

The tests were documented with real time and high speed ph tography. Vehicle kinematics was found by analysis of the high speed film. The vehicles tested represent a range of vehicle geometries from passenger cars to utility vehicles. The vehicle kinematics results include presentation of position, velocity, and energy profiles. The results are compared with those from the dolly rollover test at similar speeds with a similar vehicle.

Introduction

Automobile rollover accidents have been a subject of research for more than 50 years (1)*. Despite years of study, the mechanics of vehicle rollover remains poorly understood, a situation that can be attributed to the complexity of the rollover process. Many factors influ nce the likelihood of vehicle rollover, including vehicle characteristics, pre-rollover vehicle dynamic motion, and the nature of the mechanism initiating rollover. It is well known that a vehicle's propensity to rollover depends on vehicle characteristics that include geometric dimensions, inertial properties, and suspension characteristics. Pre-

*Numbers in parentheses designate references at end of paper.